USING RADAR ATTRIBUTES AND ENVIRONMENTAL PARAMETERS TO CLASSIFY DOWNBURSTS BASED ON OUTFLOW BOUNDARY SPEED

Ryan Tatasciore[1], James LaDue[2], and Lexy Elizalde-Garcia[3], Melissa Lamkin[3], Chris Spannagle[3], Stephanie Edwards[3], Alyssa Bates[3], and Samantha Boyd[3]

[1]National Weather Center Research Experiences for Undergraduates Program
Norman, Oklahoma

[2]NOAA/NWS/OCLO Warning Decision Training Division
Norman, Oklahoma

[3]Cooperative Institute for Severe and High-Impact Weather Research and Operations (CIWRO) & NOAA/NWS/OCLO Warning Decision Training Division
Norman, Oklahoma

ABSTRACT

Downbursts are especially strong, localized downdrafts within thunderstorms capable of producing damaging straight-line winds at the surface. Despite a moderate understanding of the microphysical and dynamical processes that cause downbursts, forecasting and nowcasting their winds remains challenging for National Weather Service (NWS) forecasters. Wind is more sensitive to radar issues and is often difficult to identify compared to other signatures, such as tornadoes. This paper identifies several important environmental parameters and radar attributes that can distinguish the intensities of 47 downburst-producing storms. A focus was placed on pulse storms, mainly in the Southeastern US, as they are more difficult to forecast when compared to more organized modes, such as supercells or squall lines. Using outflow boundary speed as a proxy for downburst intensity, we found a few variables with statistically significant correlation, including total totals, shear parameters, LFC height, and more. There was a poor correlation between boundary speed and more complex parameters that account for wind speed, such as the wind damage parameter (WNDG) and microburst composite (MBURST). These likely performed poorly due to the large number of null (sub-severe) cases in our dataset, as they are designed to identify severe wind potential. Radar attributes — including maximum Specific Differential Phase (KDP) values and maximum 50 dBZ heights above radar level — performed very well, further giving credit to their usability in nowcasting. We found that boundary speed can be utilized as an indicator of downburst intensity, as well as identified significant predictors that can be used to nowcast downbursts associated with pulse storms. Predictor variables we found to be statistically significant were similar to those of previous research that used wind reports as indicators of downburst strength. This research demonstrates the skill of using boundary speed to represent wind intensity, potentially reducing the need to rely on potentially biased storm reports in future work.

1. INTRODUCTION AND BACKGROUND

Downbursts are meteorological phenomena that pose significant threats to life and property. They can produce destructive straight-line winds that result from intense downdrafts within thunderstorms. These winds have been measured at speeds up to 150 miles per hour, equivalent to a strong tornado (Wakimoto 1985). Downbursts are especially dangerous to the aviation community, as they have been known to cause multiple high-profile accidents resulting in hundreds of fatalities (McCarthy et al. 2022). Outside of their more well-known effects on aviation, downbursts tend not to garner the same amount of public attention as other meteorological hazards, such as tornadoes or flooding events. However, straight-line winds are a much more common occurrence than tornadic winds, with 10-20 wind damage reports per one tornado report for an average year (SPC 2024). Given their higher frequency and sometimes comparable intensity, downbursts can be just as dangerous as tornadoes.

A downburst has been defined as a negatively buoyant downdraft from a thunderstorm that reaches the ground and spreads out (Fujita 1985). The word downburst is a more general term that includes both microbursts and macrobursts, which are downbursts with a horizontal extent smaller or larger than 4 km, respectively (Fujita 1985). This paper will not differentiate between the two, given their similar characteristics (besides size).

Downbursts form in a variety of storm modes and environments by any processes that contribute to a downward acceleration of an air column. Melting hail, evaporation, and precipitation loading—the drag force behind large amounts of falling rain or hail, causing air

[1] *Corresponding author address:* Ryan Tatasciore, University of Delaware, 2325 Radka Ln, Wilmington, DE, 19810. ryantat@udel.edu

to fill in behind it and accelerate downwards—are a few microphysical processes that have been previously found to accelerate a downburst (e.g., Srivastava 1987; Eilts and Doviak 1987). The initial availability of atmospheric moisture also aids downburst formation, providing more potential for latent heat release from phase changes (James and Markowski 2010). Dry air entrainment at mid-levels has also been found to aid downburst development, allowing for higher evaporation rates (Pryor 2014).

Despite a solid understanding of the physics behind downbursts, they are still very difficult to forecast, especially on days with weak synoptic forcing. Storms in these low-shear environments are referred to as pulse thunderstorms due to the brief surge in updraft, or pulse, at the onset of deep, moist convection. (Miller and Mote 2018). These pulse storms often evolve quickly and can produce damaging winds just minutes after formation, providing narrow windows of opportunity for forecasters to issue timely warnings. Additionally, radar-based signatures for impending straight-line winds are sometimes difficult to identify, especially for weak storms at a further distance from the radar site. Severe thunderstorm warnings for pulse storms in the US are generally less accurate with larger false alarm ratios and smaller probabilities of detection when compared with more organized modes such as squall lines or supercells (Guillot et al. 2008). The key motivators of this research are the present forecasting and nowcasting challenges that warning decision makers face.

This paper will analyze a variety of past downburst events and attempt to correlate near-storm environmental parameters and radar attributes to downburst strength. The focus will be on pulse thunderstorms in low-shear environments because of the stated prediction difficulties. We hypothesize that outflow boundary speed is significantly correlated with one or more independent variables. To our knowledge, this would be the first work to use outflow boundary speed as a predictand, as most previous work has used wind reports. Predictor variables that are found to be statistically significant in this paper will be compared to previous findings to assess the similarities and differences in using boundary speed as the predictand. The goal is that the findings highlight important precursors useful for operational forecasters in severe thunderstorm warning (SVR) decision-making and assess the feasibility of using boundary speed as an indicator of downburst intensity.

2. PREVIOUS RESEARCH

Past literature has investigated the atmospheric environments that support downbursts as well as radar precursor signatures to improve forecasting (e.g., Wakimoto and Bringi 1987; Kuster et al. 2016). Environmental conditions that favor a wet downburst include a mid-level dry layer, moderate to high convective available potential energy (CAPE), and steep lapse rates (Kuster et al. 2016; Romanic et al. 2022). Past radar-based studies have identified descending reflectivity cores, mid-level convergence, and differential reflectivity (ZDR) troughs as reliable indicators of an impending downburst (e.g., Isaminger 1988; Roberts and Wilson 1989; Kuster et al 2016; Miller and Mote 2017). These studies have identified these radar precursors and environmental conditions as being favorable for the development of downbursts, but had more difficulty differentiating weak downbursts from strong ones. This challenge is another key motivation for this paper.

A study that addressed this issue is Kuster et al.'s (2021) analysis of specific differential phase (KDP) values—a derived radar product that depicts the change in the differential phase shift, providing information about the shape and concentration of radar targets—associated with downburst-producing storms before the downburst occurrence (Kumjian 2013). High KDP values are indicative of large amounts of melting hail: one of the main processes that can enhance a downdraft. All 81 downbursts in the study by Kuster et al. were associated with a KDP core, and only two KDP cores were not associated with a downburst. The authors also found a positive correlation between the maximum KDP value within the core and the core's size just below the environmental melting layer (EML) with the impending downburst's intensity. However, they noted that there is a large overlap between KDP core magnitude and the strength of the downburst, meaning that stronger (weaker) KDP cores also have occurred with weaker (stronger) downbursts. While the size of the KDP core performed better to differentiate between strong and weak downbursts, it is not as operationally feasible to assess during nowcasting as other characteristics. Kuster et al. noted that KDP values themselves are not sufficient to forecast the corresponding downburst intensity and should be used in tandem with other radar signatures and near-storm environmental parameters. We will assess the skill of using maximum KDP values near the melting layer as one of our predictor variables for this dataset.

Downburst detection itself, in addition to forecasting, can be challenging. Near-surface velocity divergent signatures are only visible at close distances to radar. Sherburn et al. (2021) addressed this issue by calculating wind gust ratios (WGRs), in which the numerator is the storm's measured wind gust speed and the denominator is the speed of the outflow boundary, also referred to as the gust-front. They found few cases where the recorded wind gust was less than the speed of the gust-front, meaning forecasters can safely assume the associated wind gusts from a storm will be at least the magnitude of the gust-front's speed. The variability of the WGRs decreased substantially with increasing boundary speed, providing further confidence that storms with higher outflow boundary speeds will have stronger accompanying wind gusts. WGRs were also higher for isolated cells than linear cases, which is applicable to this paper since it will be focusing on pulse

storms. A benefit to using the gust front method is that its speed can be calculated using base radar data and only requires two scans. The gust-front is observable on radar over most viewing angles and is only dependent on range.

3. DATA AND METHODS

a. Data collection

Data were collected for this study by manually collecting downburst cases and analyzing the corresponding radar information and near-storm environment. Storm instances were found using the Storm Events Database from the National Centers for Environmental Information ((https://www.ncdc.noaa.gov/stormevents/). Storm event summaries from various National Weather Service (NWS) offices, local news reports, and often live radar data were also utilized. Only events within 100 km of a Doppler radar site were gathered, with most cases existing within 50 km. This ensured a more accurate depiction of the storm's vertical structure and allowed a clear view of the gust-front. The 100 km maximum threshold is consistent with that of Kuster et al. (2021) who performed a similar analysis.

47 wet downbursts from 11 states were analyzed during the June-September range from 2022-2024. The geographical extent is dominated by states in the Southeast US, where pulse thunderstorms most frequently occur. There are a few instances of storms in the Northeast and Midwest. However, these environments are typically higher in shear and support faster-moving storms, making it more difficult to tease out the gust-front motion from the general storm motion.

Predictor variables include 5 radar-based signatures and 23 near-storm environmental parameters. The predictors used are listed in Table 1, with descriptions and sources included. The speed of the downburst's resulting outflow boundary, also referred to as the gust-front, will be the predictand to represent the intensity of the downburst. Sherburn et al. (2021) found that the outflow boundary speed is a reasonable minimum threshold for a corresponding wind gust, as discussed in the literature review.

Past radar imagery was obtained through Amazon Web Services' WSR-88D Level II S3 explorer (https://s3.amazonaws.com/noaa-nexrad-level2/index.html). At least thirty minutes of radar data before and after the storm report was downloaded to get an accurate depiction of the evolution of the downburst. This time frame varied depending on the strength and corresponding lifespan of the storm and was sometimes extended up to an hour or more before downburst occurrence.

Table 1. Predictor variables analyzed, along with a description and reference (if applicable)

Environmental Parameter (units)	**Description (source)**
ML LCL (ft)	Mean-layer lifted condensation level
ML LFC (ft)	Mean-layer level of free convection
ML EL (ft)	Mean-layer equilibrium level
ML CAPE (J kg^{-1})	Mean layer convective available potential energy
SFC CAPE (J kg^{-1})	Surface-based convective available potential energy
DCAPE (J kg^{-1})	Downdraft convective available potential energy (Gilmore and Wicker 1998)
ML CINH (J kg^{-1})	Mean-layer convective inhibition
LowRH (%)	Mean relative humidity over the lowest 150 mb
MidRH (%)	Mean relative humidity over a layer 150-300 mb above the surface
DownT (°F)	Downrush temperature (Gilmore and Wicker 1998)
TEI (unitless)	Theta-e index (Hart and Korotky 1991)
SigSvr ($m^3 s^{-3}$)	Significant severe (Craven and Brooks 2004)
SHIP (unitless)	Significant hail parameter (SPC)
PW (in)	Precipitable water vapor below 400 mb (Hart and Korotky (1991)
MBURST (unitless)	Microburst composite (NWSFO Jackson MS)
WNDG (unitless)	Wind damage parameter (SPC)
EBWD Shear (kt)	Effective bulk wind difference (Thompson et al. 2007)
0-3 SRW (kt)	Surface to 3 km storm relative wind magnitude (Rasmussen and Blanchard 1998)
0-1 Shear (kt)	Surface to 1 km wind shear (Rasmussen 2003)
TT (unitless)	Total totals (Hart and Korotky 1991)
WB0 Level	Height at which the wet-bulb temperature is 0 ℃
Freezing Level	Height at which the environmental temperature is 0 ℃
0-6 MnWind magnitude (kt)	Surface to 6 km pressure-weighted mean wind (Rasmussen and Blanchard 1998)
Radar Attribute (units)	**Description (source)**
Max Height 50 dBZ ARL (ft)	Maximum height above radar level of 50 dBZ reflectivity values
Max Midlevel ΔV (kt)	Maximum mid-altitude radial convergence difference (Eilts et al. 1996)
Max KDP near WB0 (o km-1)	Maximum KDP value near wet-bulb zero height
Reflectivity at Max KDP at WB0 (dBZ)	Reflectivity value at the same location as above
Max KDP at 0.5 Tilt (o km-1)	Maximum KDP value at the lowest radar scan

The 23 variables depicting the near-storm environment were collected from BUFR soundings

derived from the Rapid Refresh (RAP) model (https://meteor.geol.iastate.edu/~ckarsten/bufkit/data/). The closest RAP sounding data to the report was used between 30 minutes and two hours between the downburst. This somewhat-flexible time range was utilized to prevent convective contamination of environmental variables and varied based on previous storm activity in the area. The sounding was picked based on its location downstream of storm motion. If the storm motion was minimal, the closest sounding to the storm was used. The RAP allows for a generally accurate depiction of the near-storm environment in most cases. However, there have been identified biases associated with the RAP model (e.g., Laflin 2013, Thompson et al. 2003). Despite this, modeled sounding data was used due to its higher spatial and temporal frequency compared to radiosonde data. Observed soundings are very geographically sparse and only occur twice a day, making them poor tools to accurately portray the specific environment around a small storm cell.

Measured wind data was collected from Automated Surface Observing Systems (ASOS), Automated Weather Observing Systems (AWOS), Mesonet, and Mesowest. Any estimated wind gust reports were not used to depict actual wind speeds given their biases (e.g, Edwards et al. 2018). Wind gust reports were associated with the downburst by aligning the time and geographic location of the report with where downburst winds likely occurred on radar. However, the wind gusts were only added to a small number of cases to be analyzed as an additional predictand.

The speed of the gust-front was calculated within the GR2Analyist software. The gust front was identified using at least one of the following radar products: reflectivity (Z), velocity (V), or spectrum width (SW). Figure 1 shows an example case. The speed of the front was measured by the simple distance over time formula. The outflow boundary was tracked starting from the frame it was easily visible. A marker was placed at the next frame and the speed was calculated. Efforts were made to ensure the gust-front was a result of the downburst itself. A velocity divergence signature was required to have occurred before the speed of the gust front was measured. However, the strength of this divergence signature was not used as an indicator of the strength of the downburst due to its high dependence on distance from the radar. Rather, its existence itself was only used to show that a downburst occurred, regardless of the maximum velocity difference (delta V) within the signature.

Using the gust front for our purposes eliminates the biases that come with relying on storm reports from the National Centers for Environmental Information (https://www.ncdc.noaa.gov/stormevents/). Often, estimated wind gusts from observers during the storm and inferred from post-event damage are not the most accurate; a study by Edwards et al. (2018) found that human-based wind estimates tend to inflate measured values by about 25%. Given the large number of weak downbursts from small pulse storms in the study, measured gusts were also difficult to obtain.

Similar to the methods of Kuster et al. (2021), the maximum KDP value for a given cell was calculated at a height around the environmental wet bulb zero level. This is the height in which falling hail would have already started to melt, accelerating the downdraft, which is depicted by the elevated KDP values found at this level. This height was identified from the thermodynamic diagram in the RAP output data. Observations of the melting layer height were confirmed by using differential reflectivity and correlation coefficient in stratiform precipitation adjacent to the downburst location. A height just below this level was given preference. However, if the closest radar scan was more than a few thousand feet below the height, the next-highest scan was used. The maximum value recorded had to occur at some point before the downburst occurrence. This ensured the fact that KDP can be used as a predictor variable, as analyzing any remaining KDP core after the fact would not be relevant to this study.

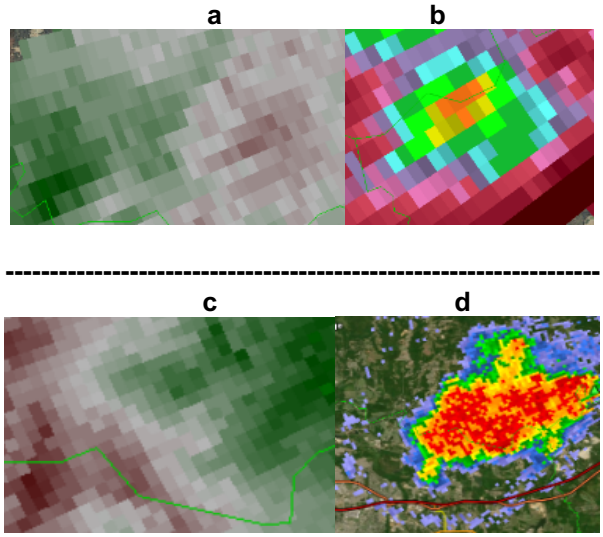

Figure 1. An example of a WSR-88D depiction of a downburst, where a) depicts mid-altitude radial convergence just below the melting level, b) depicts the KDP core at that height, c) depicts velocity divergence near the surface on the next scan, and d) depicts the gust-front on reflectivity on the subsequent scan

b. Types of analysis

The data were first analyzed using Spearman's rank correlation coefficient (CC) to compare the environmental parameters and radar attributes to outflow boundary speed. Spearman's CC was used instead of Pearson's since it is more resistant to outliers, which exist toward the upper bounds of this dataset (Schober et al. 2018). It converts the dataset into ranks and then performs Pearson's method. The CC was

calculated between every predictor variable (environmental and radar) and outflow boundary speed.

The t-test was also utilized to compare the difference in the means of the predictor variables between the higher and lower ends of outflow boundary speeds. Welch's t-test was used rather than student's because it is also more resistant to slightly non-normal distributions (West 2021). The data were divided into boundary speeds below and above the interquartile range (IQR), corresponding to speeds less than 13 knots (weak) and greater than 24 knots (strong). While these groups naturally have smaller sizes than splitting the data, say, in half, it was done to make any relationships more clear. Once divided, the t-test was performed to determine which predictor variables best differentiated between slower and faster boundary speeds. These divider values were chosen based on the distribution of the data collected, rather than meteorological benchmarks, such as severe vs non-severe winds. This was because a) we used boundary speed instead of measured gusts and b) most of the storms in the dataset were not associated with severe reports. Dividing the data into quartiles allowed for similar variances and ensured equal representation of both sides. For example, we could also have split the data based on the criteria for severe wind, which is 50 kts. Using Sherburn et al.'s (2021) findings of an average WGR for disorganized storm modes of 1.8, the corresponding gust-front speed would be about 28 kts. In this dataset, there are only six downbursts that produced severe-worthy boundary speeds. Therefore, the data was split based on its own characteristics, rather than severe vs non-severe.

4. RESULTS AND DISCUSSION

a. Environmental parameters

Parameters that correlated the best with outflow boundary speed included the total totals (TT) index, measurements of shear, the SigSvr index, mixed-layer (ML) convective inhibition (CINH), the level of free convection (LFC), and the significant hail parameter. A couple variables that performed unexpectedly poorly included the wind damage parameter (WNDG) and the microburst composite (MBURST), and precipitable water (PW). Figure 2 shows the best-performing environmental parameters according to the t-test. It surprised us that TT performed as well as it did, given its age and relative simplicity when compared to other environmental parameters (Table 2) For example, it only considers temperature and dew point at two fixed levels, while the equation for the MBURST index contains eight different variables. Interestingly, Miller and Mote (2018) similarly found that VT and TT were the only two variables to appreciably differentiate severe wind supporting days for weakly forced thunderstorms. As those authors noted, this may be due to the reduced model error in this parameter given its simplicity when compared to other more complex indices. When compared to observed soundings, TTs were represented by the model with a less than 1 degree C bias (Miller and Mote 2018). Regardless, the fact that their study also found TT to perform well gives credibility to using outflow boundary speed as a representation of downburst intensity.

Table 2. Predictor variables correlated with outflow boundary speed, sorted by ascending p-values

Environmental Parameter	Average	Spearman Correlation	P-value
TT	47.19	0.5275	0.0001
ML CINH	6.17	0.5124	0.0002
LFC (ML)	1537	0.5050	0.0003
0-6 MnWind	9.49	0.4582	0.0012
EBWD Shear	14.6	0.4437	0.0018
LowRH	66.3	-0.3982	0.0056
ML LCL	1375	0.3592	0.0132
SigSvr	17738	0.3259	0.0254
SHIP	0.33	0.2712	0.0652
0-1 Shear	5.21	0.2263	0.1261
DCAPE	1080	0.2253	0.1278
Freezing Level	15740	-0.1916	0.1970
SFC CAPE	2926	-0.1500	0.3142
0-3 SRW	15.79	0.1165	0.4355
MidRH	69	-0.0987	0.5093
WNDG	0.40	0.0854	0.5682
WB0 Level	12785	0.0691	0.6443
EL (ML)	13660	-0.0642	0.6681
DownT	64.34	-0.0436	0.7710
PW	1.89	0.0311	0.8357
ML CAPE	2355.	-0.0201	0.8935
TEI	29.57	-0.0128	0.9320

MBURST	3.06	0.0036	0.9807

Radar Attribute	Average	Spearman Correlation	P-value
Max height 50 dBZ ARL	29183	0.613	4.72E-06
Max Mid-Level ΔV	17.29	0.469	0.00089
Max KDP value at WB0 Level	5.08	0.468	0.00091
Max KDP at 0.5 Tilt	4.11	0.263	0.07426
Reflectivity at Max KDP Value at WB0	57.59	0.032	0.8310

We were initially surprised that higher absolute values of ML CINH were associated with stronger storms. While higher convective inhibition may impede the initial formation of storms, our data did not include cases without storm formation. The higher CINH values may have allowed for more potential energy near the surface to build up throughout the day, leading to a stronger updraft and corresponding downdraft. A similar argument can be made regarding the positive correlation with LCL and LFC heights. A higher LFC corresponds with a higher LCL, enabling a deeper dry layer for downdraft acceleration.

Atmospheric wind indices, such as bulk wind difference (EBWD) and 0-6 km mean winds, were top distinguishers between weaker and stronger outflow boundary speeds. Elevated levels of shear can enhance downburst strength by transporting drier air into the mid-levels of the storm, leading to stronger evaporative cooling and enhancing the downdraft (Wakimoto and Bringi 1987). Since most of our cases were composed of lower-shear environments (average EBWD shear of 14 kts), it is likely an analysis of higher shear environments would contain storms with higher boundary speeds.

It is possible the indices specifically designed for wind damage, such as WNDG and MBURST, performed poorly in this dataset due to the majority of cases being sub-severe. These parameters may be better at differentiating between days that support potential for severe winds, rather than differentiate between a 20 and 30 knot wind gust, for example. Miller and Mote (2018) note that the research used to develop new parameters often contains relatively small ratios of non-severe cases. Additionally, of the seven environmental parameters included in the pulse downburst study by Kuster et al. (2021), MBURST also was also the worst performer. In their study the p-value was 0.1178, with the next-highest being 0.0196, when looking at favorable and non-favorable environments for high KDP values. These indices have performed better in a dataset with a higher number of severe storms (Miller and Mote 2018).

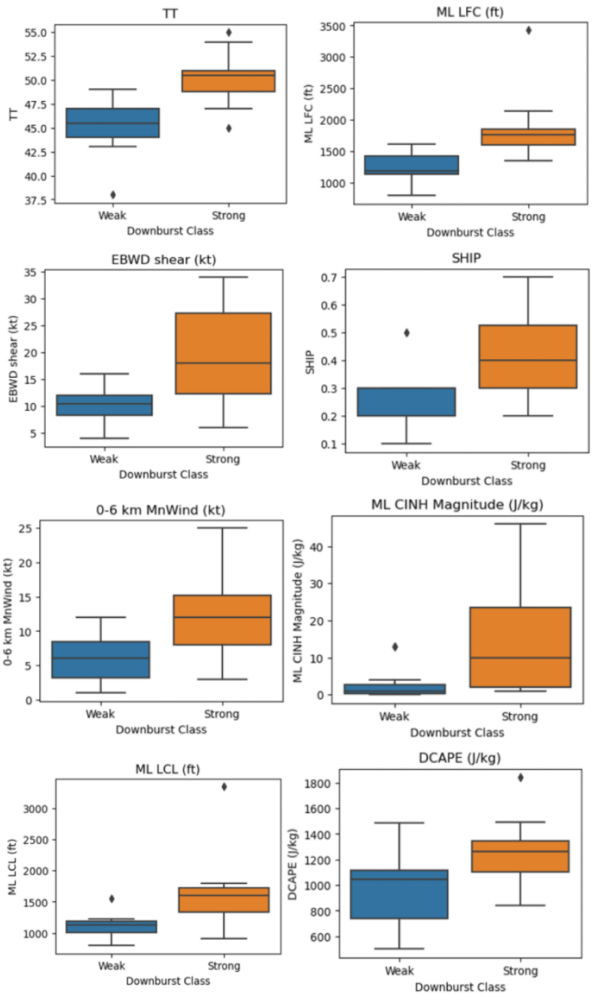

Figure 2. Statistically significant (>95% confidence) environmental parameters when using the t-test to compare weak (<13 kt) and strong (>24 kt) outflow boundary speeds

b. Radar attributes

Figure 3 shows the best performing radar attributes according to the t-test. Of the radar attributes analyzed, the maximum height of 50 dBZ above radar level (ARL) performed the best, according to Spearman's CC. This attribute also did the best in discriminating between the means of the upper and lower quartiles, according to the t-test. High reflectivity values at high altitudes are indicative of large hydrometers that have reached upper levels in the atmosphere. This is indicative of a strong updraft within the storm and allows for a stronger corresponding downdraft. From a higher elevation, the downdraft has more vertical distance to gain strength and will be stronger at the surface.

Mid-altitude radial convergence (MARC), or delta V, was also positively correlated with boundary speed, having the second highest CC. This trait was determined to be an important sign of an impending downburst by Eilts et al. (1996). Convergence aloft occurs as air rushes in to replace the empty space left by the collapse of the air column (the downburst). Since this takes a few minutes to reach the ground, the MARC signature at mid-levels is a key signature that a downburst will occur shortly after.

Finally, the KDP core maximum just below the melting layer, and near the surface, also performed well. This further validates the findings from Kuster et al. (2021) that KDP cores can act as another downburst precursor, starting at high elevations and collapsing downward. Every downburst storm in this dataset contained a KDP core at some point before its occurrence. Timewise, the maximum KDP value was recorded, on average, 15 minutes before the outflow boundary speed measurement was taken. In our case, this time value is an upper bound, since the outflow boundary is only apparent after the downburst has already hit the surface and has spread out. So, the likely actual timing of the downburst is a frame or two before the boundary speed measurement was taken.

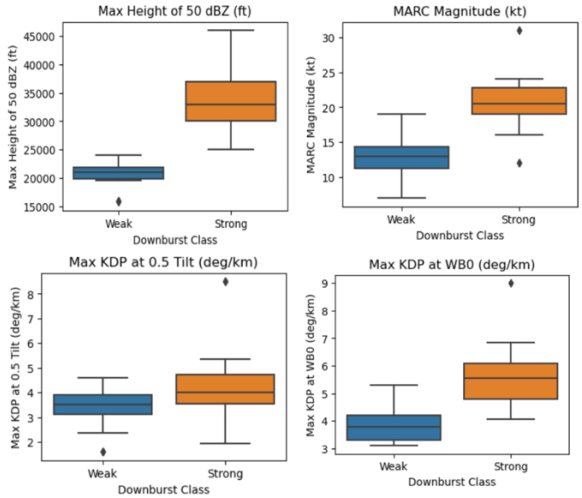

Figure 3. As in Figure 2, but for radar attributes.

c. *Reports subset*

Of the 47 instances in the dataset, 14 included measured wind gusts. Similar analysis was performed on this subset, this time using the measured wind gust as the predictand rather than outflow boundary speed. The only predictor variable across both environmental and radar that correlated with 95% confidence or greater was DCAPE. Additionally, when correlated with outflow boundary speed itself, there was no clear relationship. While the DCAPE correlation makes sense given this parameter's use in forecasting winds from downdrafts, the measured wind gusts did not correlate well generally. The extremely small sample size could be to blame for the lack of meaningful relationships. Future research may include wind records for a larger ratio of cases in the dataset and attempt to analyze correlations with boundary speed for a more thorough analysis.

The data were also split into those with damage reports, and a second null group. A little less than half (22 of the 47) storms had wind damage reports associated with them. The reports varied from branches down to sheds blown away. The average outflow boundary speed for this group was 19.4 knots, compared to 16.3 knots for the other 25 storms without reports. The top-performing environmental parameters looked similar, but one notable difference was the increase in the performance of MBURST and WNDG. They both exhibited a weak but negative correlation with outflow boundary speed for the group without reports, and a weak but positive correlation for the group with reports. This increase is visualized in Figure 4. However, the large scatter in both plots shows the overall mediocre performance of these parameters. Forecasters should use these indices with caution and consider additional parameters when preparing for downburst occurrences.

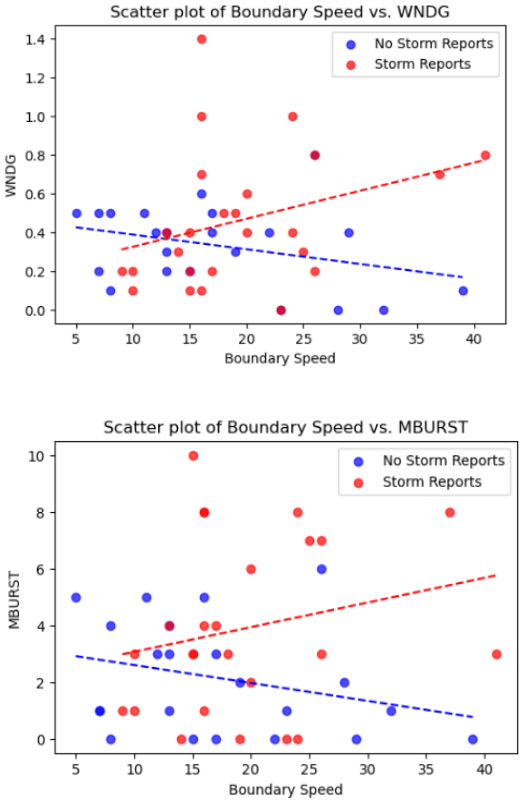

Figure 4. Scatterplot of MBURST composite and WNDG parameter when compared to outflow boundary speed. The red represents downbursts with associated storm damage reports, while the blue represents those without.

5. CONCLUSIONS

This research tested the ability of radar precursors and modeled environmental parameters to represent the strength of the impending downburst, as quantified by its resulting outflow boundary speed. Using boundary speed allowed us to rely on a variable that is easily measured from radar and takes away the need to rely on potentially biased ground reports or measurements. We analyzed mainly pulse thunderstorms in weakly-forced environments, as they have been historically underrepresented in research yet are some of the most challenging meteorological phenomena to forecast. We found the following:

- The environmental variables best correlated with boundary speed across the dataset included total totals, convective inhibition, effective bulk wind difference, 0-6 km mean winds, LFC height, and the SigSvr index.

- Environmental parameters that performed surprisingly poorly included WNDG and MBURST parameters. The values of these variables did not differentiate between weaker and stronger downbursts, as classified by outflow boundary speeds. They performed better on stronger downbursts associated with damage reports and may demonstrate more skill in a dataset with a higher ratio of severe wind-producing downbursts.

- Radar attributes performed very well. KDP values below the melting level (and subsequently at the lowest scan), mid-level radial convergence, and the maximum height of 50 dBZ reflectivity ARL were all positively correlated with boundary speed with high (>95%) confidence. When comparing t-test values for the upper and lower quartiles, three of the five radar attributes analyzed appeared in the top five best differentiators between weak and strong boundary speeds across all 28 environmental and radar predictor variables.

- When testing the skill of the predictor variables with the subset of 14 instances with measured wind gusts, DCAPE was the only variable that demonstrated skill when wind gust speed was the predictand. Boundary speed itself also did not correlate with the measured wind gusts. However, given the extremely small size of this subset, conclusions from this subset should be used with hesitation.

One of the questions that encouraged this research was the usability of boundary speed as the predictand for wind speeds. To address this, we can compare the variables that we found to be statistically significant using boundary speed to those from previous research that used storm reports instead of boundary speed. Total totals stuck out the most, being the best differentiator for Miller and Mote 2018 and for this research. Additionally, parameters that demonstrated the most skill in the downburst analysis by Romanic et al. (2022) included cold pool strength, DCAPE, LCL and LFC height, and low-level lapse rates. These parameters also performed well in our dataset.

There are a handful of noteworthy limitations to this study. The small sample size (<50) could have inflated the effect of outliers, making the trends generally less reliable. However, this number was the largest number of cases we could collect in the limited timeframe. Additionally, model biases may have influenced the findings. For example, TT was found to be the best correlated environmental parameter, and it is also associated with the least amount of error in RAP modeled soundings. Finally, the measured speed of the outflow boundary had some variability and was sensitive to the location marked on the gust-front. The error for each measurement is likely a few knots, but the effect of this would likely be reduced using a larger dataset.

Future work may aim to incorporate outflow boundary speed for a larger and more diverse dataset. Machine learning (ML) and algorithms could be trained to detect downbursts and measure the corresponding boundary speed from radar data. This could reduce the need for storm reports or wind measurements to confirm a downburst occurred. The only limitation would be distance from the nearest radar, as the boundary must be visible on at least one radar product. A similar study using downbursts from across the country in a variety of storm modes would likely result in more trustworthy and comprehensive results regarding why some downbursts are much more severe than others.

Despite the challenges, the predictor variables we found to be significant when related to outflow boundary speed are similar to those analyzed in previous studies that used storm reports. This suggests that boundary speed has potential to be used as a predictand representing the intensity of a downburst and possibly the strength of the corresponding straight-line winds. The performance of radar attributes, such as KDP values and the MARC signature, further demonstrates their usability in nowcasting, even for non-severe storms. Forecasters can have increased confidence that a downburst will occur given overlapping radar signals, such as a strong KDP core combined with a high 50 dBZ height. While distinct thresholds for these values that can differentiate between a non-severe and downburst-producing storm were not created by this study, we highlight the relative skill of each parameter compared to the outflow boundary speed. Hopefully, this research opens the door for further studies to utilize outflow boundary speed to categorize a larger sample of downbursts. This may correlate additional precursors or confirm ones found to

be significant in this study to give forecasters more tools to warn of potentially damaging straight-line winds.

Acknowledgments. The authors would like to thank Dr. Daphne LaDue and Alex Marmo for their hard work in running another year of REU. This work was prepared by the authors with funding provided by National Science Foundation Grant No. AGS-2050267, and NOAA/Office of Oceanic and Atmospheric Research under NOAA-University of Oklahoma Cooperative Agreement #NA11OAR4320072, U.S. Department of Commerce. The statements, findings, conclusions, and recommendations are those of the author(s) and do not necessarily reflect the views of the National Science Foundation, NOAA, or the U.S. Department of Commerce.

6. REFERENCES

Amazon Web Services, 2024: AWS S3 Explorer. https://s3.amazonaws.com/noaa-nexrad-level2/index.html (Accessed July 30, 2024)

Craven, J.P. & Brooks, Harold, 2004: Baseline climatology of sounding derived parameters associated with deep, moist convection. Natl. Wea. Dig.. 28. 13-24.

Edwards, R., J. T. Allen, and G. W. Carbin, 2018: Reliability and Climatological Impacts of Convective Wind Estimations. J. Appl. Meteor. Climatol., 57, 1825–1845

Eilts, M. D., and R. J. Doviak, 1987: Oklahoma Downbursts and Their Asymmetry. J. Appl. Meteor. Climatol., 26, 69–78

Fujita, T.T., 1985. The Downburst: Microburst and Macroburst. Satellite and Mesometeorology Research Project. Department of the Geophysical Sciences, University of Chicago, 136

Fujita, T.T., 1985. The Downburst: Microburst and Macroburst. Satellite and Mesometeorology Research Project. Department of the Geophysical Sciences, University of Chicago, 136

Gilmore, M. S., and L. J. Wicker, 1998: The Influence of Midtropospheric Dryness on Supercell Morphology and Evolution. *Mon. Wea. Rev.*, **126**, 943–958

Guillot, E. M., Smith, T. M., Lakshmanan, V., Elmore, K. L.,Burgess, D. W., and Stumpf, G. J.: Tornado and severe thunderstorm warning forecast skill and its relationship to storm type, in: 24th Int. Conf. Interactive Information Processing Systems for Meteor., Oceanogr., and Hydrol., New Orleans, LA, 4A.3,

Hart, J. A., and W. Korotky, 1991: The SHARP workstation v1.50 users guide. National Weather Service, 30 pp.

Isaminger, M. A., 1988: A preliminary study of precursors to Huntsville microbursts. Lincoln Laboratory Project Rep. ATC-153, 22

Iowa State University, 2024: The BUFKIT Warehouse. https://meteor.geol.iastate.edu/~ckarsten/bufkit/data/ (Accessed July 30, 2024)

James, R. P., and P. M. Markowski, 2010: A Numerical Investigation of the Effects of Dry Air Aloft on Deep Convection. Mon. Wea. Rev., 138, 140–161

Kumjian, M. R., 2013: Principles and applications of dual-polarization weather radar. Part I: Description of the polarimetric radar variables. J. Operational Meteor., 1 (19), 226242

Kuster, C. M., P. L. Heinselman, and T. J. Schuur, 2016: Rapid-Update Radar Observations of Downbursts Occurring within an Intense Multicell Thunderstorm on 14 June 2011. Wea. Forecasting, 31, 827–851

—. M., B. R. Bowers, J. T. Carlin, T. J. Schuur, J. W. Brogden, R. Toomey, and A. Dean, 2021: Using KDP Cores as a Downburst Precursor Signature. Wea. Forecasting, 36, 1183–1198

Laflin, Jennifer, 2013: Verification of RAP Model Soundings in Preconvective Environments. Journal of Operational Meteorology. 1. 66-70. 10.15191/nwajom.2013.0106.

McCarthy, J., R. Serafin, J. Wilson, J. Evans, C. Kessinger, and W. P. Mahoney, 2022: Addressing the Microburst Threat to Aviation: Research-to-Operations Success Story. Bull. Amer. Meteor. Soc., 103, E2845–E2861

Miller, P.W., Mote, T.L., 2018. Characterizing severe weather potential in synoptically weakly forced thunderstorm environments. Nat. Hazards Earth Syst. Sci. 18, 1261–1277

NOAA, National Centers for Environmental Information, 2024: Storm Events Database. https://www.ncdc.noaa.gov/stormevents/ (Accessed July 30, 2024)

Pryor, Kenneth. (2014). Downburst Prediction Applications of Meteorological Geostationary Satellites. Proceedings of SPIE - The

International Society for Optical Engineering. 9259. 10.1117/12.2069283.

Schober, Patrick MD, PhD, MMedStat; Boer, Christa PhD, MSc; Schwarte, Lothar A. MD, PhD, MBA. Correlation Coefficients: Appropriate Use and Interpretation. Anesthesia & Analgesia 126(5):p 1763-1768, May 2018

Rasmussen, E. N., and D. O. Blanchard, 1998: A Baseline Climatology of Sounding-Derived Supercell and Tornado Forecast Parameters. *Wea. Forecasting*, **13**, 1148–1164

---, E. N., 2003: Refined Supercell and Tornado Forecast Parameters. *Wea. Forecasting*, **18**, 530–535

Roberts, R. D., and Wilson J. W. , 1989: A proposed microburst nowcasting procedure using single-Doppler radar. J. Appl. Meteor., 28, 285–303

Romanic, D., Taszarek, M. Brooks, H., 2022: Convective environments leading to microburst, macroburst and downburst events across the United States. Weather and Climate Extremes, 37, 100474

Sherburn, K. D., M. J. Bunkers, and A. J. Mose, 2021: Radar-Based Comparison of Thunderstorm Outflow Boundary Speeds versus Peak Wind Gusts from Automated Stations. Wea. Forecasting, 36, 1387-1403

Srivastava, R. C., 1985: A Simple Model of Evaporatively Driven Downdraft: Application to Microburst Downdraft. J. Atmos. Sci., 42, 1004–1023

Storm Prediction Center, 2024: SPC Storm Reports. https://www.spc.noaa.gov/climo/reports/ (Accessed July 30, 2024)

Thompson, Richard & Edwards, Roger & Hart, John & Elmore, Kimberly & Markowski, Paul. (2003). Close Proximity Soundings within Supercell Environments Obtained from the Rapid Update Cycle. Weather and Forecasting - WEATHER FORECAST. 18. 1243-1261.

Thompson, R. L., C. M. Mead, and R. Edwards, 2007: Effective Storm-Relative Helicity and Bulk Shear in Supercell Thunderstorm Environments. *Wea. Forecasting*, **22**, 102–115

University of Oklahoma, 2024: SHARPy. https://sharp.weather.ou.edu/dev/ (Accessed July 30, 2024)

Wakimoto, R. M., 1985: Forecasting dry microburst activity over the High Plains. Mon. Wea. Rev., 113, 1131-1143.

Wakimoto, R. M., and V. N. Bringi, 1987: Dual-Polarization observations of Microbursts Associated with Intense Convection: The 20 July Storm during the MIST Project. Mon. Wea. Rev., 116, 1521–1539

West RM, 2021. Best practice in statistics: Use the Welch t-test when testing the difference between two groups. Annals of Clinical Biochemistry., 58(4):267-269